Journal of Marine Research, 66, 441–463, 2008

An estimate of Lagrangian eddy statistics and diffusion in the mixed layer of the Southern Ocean

by J. B. Sallée[1,2], Kevin Speer[3], R. Morrow[1] and R. Lumpkin[4]

ABSTRACT

A statistical analysis of surface drifter observations is used to compute eddy length and time scales and eddy diffusion in the Southern Ocean. Eddy diffusion values of the order of 10^4 m^2 s^{-1} are found in the energetic western boundary currents north of the Antarctic Circumpolar Current (ACC) and secondary peaks occur where the ACC negotiates topography. The diffusivity shows an increase from the Antarctic continent to the core of the ACC, then a slight decrease or a stable plateau within the ACC. North of the ACC, diffusivity generally decreases into the interior of ocean basins, except in the western boundary regions where values are maximum.

Diffusivity is also calculated from simulated trajectories based on altimetric geostrophic velocities, with and without mean flow, as well as with simulated trajectories based on Ekman currents. Ekman currents at the drogue depth (15 m) have only a small impact, and the geostrophic currents dominate the eddy diffusivity. Complementary statistical analyses confirm these results. The surface drifter cross-stream eddy diffusion is used to test a simple parameterization based on satellite altimetric observations of eddy kinetic energy (EKE). For $EKE \geq 0.015$ m^2 s^{-2}, $\kappa = 1.35\sqrt{EKE}L_d$ m^2 s^{-1}, where L_d is the first baroclinic Rossby radius. This parameterization holds in the energetic ACC, consistent with an eddy field in the "frozen field" regime. Over the broader areas of weaker eddy fields, mixing is fairly uniform and stable at about $\kappa = 1800 \pm 1000$ m^2 s^{-1}.

1. Introduction

Knowledge of the mechanisms controlling the transport and mixing of mixed layer properties by mesoscale eddies is of primary importance to our understanding of the general circulation of the ocean. An accurate parameterization of the effect of these eddies on the large-scale circulation is fundamental for climate models as well as for *in-situ* studies of dynamic processes. However, such parameterizations are often poorly justified by observational data due to the difficulties in observing these effects. Eddies drive fluid particles in a complex evolution, straining and distorting the flow. As it is difficult to describe mathematically all of the components of such an evolution it has long been accepted that a useful framework for eddy effects on the larger-scale flow is a statistical one.

1. LEGOS-OMP, 14 Avenue Edouard Belin, 31400 Toulouse, France.
2. Corresponding author. ***email: jbsallee@gmail.com***
3. Department of Oceanography, Florida State University, Tallahassee, Florida, 32306, U.S.A.
4. NOAA/AOML, Physical Oceanography Division, 4301 Rickenbacker Causeway Miami, Florida, 33149, U.S.A.

The classical calculation of the eddy diffusion coefficient based on Lagrangian data statistics was introduced by Taylor (1921) and summarized by Batchelor and Townsend (1956). In the context of ocean circulation, Davis (1991) discussed the application of Lagrangian observations (e.g. Owens, 1984) and treated the problem of data distribution (see review by LaCasce, 2008). To produce significant results, this approach requires a substantial amount of Lagrangian data. In recent years, the steady increase in ocean subsurface floats and surface drifters has led to several studies applying the statistical formalism to ocean data, mainly in the Atlantic and Pacific oceans (e.g. Lumpkin and Flament, 2001; Lumpkin *et al.*, 2002; Bauer *et al.*, 2002; LaCasce and Bower, 2002; Oh *et al.*, 2000; Zhurbas and Oh, 2003; 2004). However, few attempts have been made to compute Lagrangian statistics in the Southern Ocean, because fewer observations existed.

Early work in the Southern Ocean was directed at the basic circulation and energetics of surface flow (Patterson, 1985). More recently, the advent of satellite altimetry has greatly improved our knowledge of the Southern Ocean surface eddy statistics (e.g. Stewart *et al.*, 1996). Keffer and Holloway (1988) and Stammer (1998) provided a global assessment of the eddy diffusion coefficient computed from an altimetric sea level product and based on scaling arguments. However these parameterizations are compromised by the fact that the diffusivity is scaled by an unknown multiplicative coefficient. Zhurbas and Oh (2004) used global surface drifter observations to estimate eddy diffusivity in the Pacific and Atlantic oceans. They found patches of intense diffusivity in all the energetic western boundary currents and in the equatorial band. For the Southern Ocean in particular they found highly diffusive areas in the Brazil Current, and in the Atlantic portion of the Agulhas Retroflection.

Marshall *et al.* (2006) developed an eddy diffusion estimate in the Southern Ocean based on the spreading of a virtual tracer whose evolution is deduced from altimetric sea-surface height data. Their results are derived formally as averages on tracer coordinates but could be displayed in geographical coordinates after some transformation. In interior and highly energetic areas (such as the Agulhas Retroflection or Brazil Current), they show weaker values than previously found with *in-situ* Lagrangian analyses (Zhurbas and Oh, 2004), or compared to diffusion in other highly energetic currents, such as the Gulf Stream (Lumpkin *et al.*, 2002) or the Kurushio (Zhurbas and Oh, 2004).

Although poorly known, eddy diffusion in the Southern Ocean has been shown to be of primary importance in climate studies. A recent study by Hogg *et al.* (2008) suggested that the eddy heat flux may contribute significantly to the observed warming of the Southern Ocean. In addition, eddy diffusion has been shown to be important in the local mixed layer heat budget and in reducing stratification in regions of the Subantarctic Mode Water (SAMW) formation in the Southern Ocean (Sallée *et al.*, 2006; 2008a). A better understanding and parameterization of surface eddy diffusion is important for upper ocean heat and salt budgets, and clearly fundamental for large-scale sea-surface temperature prediction and climate studies.

In this paper we estimate the eddy diffusion coefficient over the circumpolar Southern Ocean using the classical approach based on the statistics of surface drifter displacements.

We also attempt to understand operationally the dominant contribution to this coefficient, in terms of geostrophic and other accessible components of the flow. The statistical theory is briefly reviewed in Section 2, while the data and the practical difficulties of applying the theory to *in-situ* data are presented in Section 3. We present the results and a discussion in Section 4.

2. Background

A statistical description of the ocean is often made in terms of single particle statistics, or absolute statistics, such as means, variances and dispersion (Freeland *et al.*, 1975; Davis, 1991). These statistics are based on the probability that a given particle of the flow is found at a particular position in space, and relates to the translation of a marked fluid.

Multiple particle statistics provide a complementary description of the flow, more directly related to the distortion of the flow by shear (Bennett, 1984 and 1987). LaCasce and Bower (2000) examined relative dispersion in the ocean, especially to determine the scales of the transition from anomalous to regular dispersion. In this paper we will consider both single particle statistics and the relative dispersion of two particles in the description of the diffusivity in the Southern Ocean. Single and multiple particle statistics have been widely examined and described. Here, we present a brief summary of the terms and notations following LaCasce (2008).

Single particles. We start with the probability density function, $Q = Q(X, t)$, a function of displacement X and time t. The assumption that Q is independent of geographic position is questionable but standard; we will divide the domain into small geographic areas in which the flow is assumed to be homogeneous. The first moment of Q defines the mean displacement, $\overline{X}(t)$. The second central moment is the dispersion, $\overline{X_c^2}(t) = \overline{(X - \overline{X})^2}(t)$. The absolute diffusivity $\kappa^{(1)}$ is defined as the time derivative of the second central moment:

$$\kappa^{(1)} \equiv \frac{1}{2}\frac{d}{dt}\overline{X_c^2} \tag{1}$$

which in (well-sampled) homogeneous turbulence becomes a constant after several integral time scales.

Taylor (1921) showed that under stationary conditions the dispersion can be associated with an effective eddy diffusivity and can be written:

$$\kappa^{(1)} \equiv u_{rms}^2 \int_0^t R(\tau)d\tau, \tag{2}$$

where $u_{rms} = \sqrt{\overline{u'^2}}$ is the characteristic eddy speed, u' is the fluctuating part of the velocity, and the velocity autocorrelation function, R, is:

$$R(\tau) = \lim_{T_m \to \infty} \frac{1}{u_{rms}^2 T_m} \int_0^{T_m} u'(t)u'(t+\tau)dt. \tag{3}$$

Consequently, the dispersion can be written:

$$\overline{X_c^2}(t) = 2u_{rms}^2 \int_0^t (t-\tau)R(\tau)d\tau. \tag{4}$$

The characteristic timescale of dispersion is the Lagrangian time scale: $T = \int_0^\infty R d\tau$. This is the lag over which the motion of a particle remains strongly correlated with itself. This timescale may be converted to a distance called the Lagrangian eddy length scale, $L = u_{rms}T$. At short time scales, i.e. $t \ll T$, $R(t) \approx 1$, and the dispersion grows quadratically in time. At longer scales, when $t \gg T$, if the integral converges, then the dispersion grows linearly in time. Consequently, the diffusivity asymptotes to $\kappa_\infty^{(1)} = u_{rms}^2 T$ (Davis, 1982).

Multiple particles. Consider two particles at position x_1 and x_2. We define their reference position $x \equiv x_1$ and separation $y \equiv x_2 - x_1$. Let Q(x,y,t | x_0, y_0, t_0) be the probability that two particles, initially at x_0 with separation y_0, will move to x at time t with a separation y. As with the single particle statistics, we can define their relative dispersion by the second central moment of Q, $\overline{Y_c^2}(t) = \overline{(Y-\overline{Y})^2}(t)$. Hence, the relative diffusion is defined as the temporal derivative of the relative dispersion:

$$\kappa^{(2)} \equiv \frac{1}{2}\frac{d}{dt}\overline{Y_c^2}. \tag{5}$$

When the separation is small, the relative dispersion grows quadratically. When the particle separation is large, the relative diffusion approaches twice the absolute diffusion: $\kappa_\infty^{(2)} = 2\kappa_\infty^{(1)}$ (LaCasce, 2008). Both single and multiple particle estimates are made in the following sections.

3. Data and methods

In the first part of this study we use satellite-tracked surface drifter data to derive an assessment of the absolute diffusivity and eddy length scales in the Southern Ocean. We also use altimetry to simulate drifter trajectories. The advantage of simulating drifter trajectories using altimetry is that we overcome the problems of the irregular distribution of real drifter data in the ocean. We also reduce the noise of the aliased small-scale phenomena in the drifter measurement (e.g. inertial waves). Finally we can estimate the role of the mean flow on the eddy diffusion by simulating drifters with and without a mean flow. We also assess the contribution of the Ekman component of the velocity to the eddy diffusion by simulating drifters advected only by the Ekman flow.

In this section we present the datasets we have used, the problems in applying the theory to each dataset, and the solutions we have chosen to resolve these problems.

a. Global Drifter Program drifters

We use satellite-tracked surface drifter data from the Global Drifter Program (GDP, Lumpkin and Pazos, 2007) to compute the Lagrangian statistical formulation presented

previously. This dataset spans the period 1995-2005 in the Southern Ocean. The drifters are equipped with a holey sock drogue at 15 m depth to reduce their surface wind drag (Sybrandy and Niiler, 1991). The data are received, processed and distributed by the Atlantic Oceanographic and Meteorological Laboratory (AOML, Miami).[5] Drifters operating at a duty cycle of 1/2 or less were excluded from our analysis. Drifters having lost their holey sock drogue were also dropped from our calculation for this study. Velocities $\mathbf{u}$ were calculated from 6-hourly interpolated positions (Hansen and Poulain, 1996) via a 12-hour centered difference. Residual velocities $\mathbf{u}' = \mathbf{u} - \mathbf{U}_s$ were calculated with respect to seasonal mean currents $\mathbf{U}_s$, the latter calculated from drifter observations at a resolution of 1° using the technique of Lumpkin and Garraffo (2005)[6] and mapped onto the 6-hourly positions via linear interpolation. The Lagrangian time series of residual speeds for each drifter was low-pass filtered to remove energy at periods smaller than two days, e.g., inertial and tidal oscillations, using a second order Butterworth filter. Trajectories shorter than six days were discarded.

b. Altimetry

In order to simulate drifters in the Southern Ocean we have constructed weekly maps of Sea-Surface Height referenced to 1500 m ($SSH_{1500\mathrm{m}}$) from 1993 to 2005. Specifically, we add the mean dynamic height computed from a historical database relative to 1500 m using ship and Argo float data (Sallée *et al.*, 2008b) to the weekly maps of altimetric sea level anomalies, SLA. The mapped SLA fields are provided by CLS/AVISO and are based on data from the available altimeter missions (Topex/POSEIDON, ERS-1 and ERS-2, GFO, ENVISAT, JASON). The mapping technique is described by LeTraon *et al.* (1998). Anomalies are calculated with respect to a 7-year mean (1993-1999) and are mapped onto a 1/3° grid in longitude and variable grid in latitude, ranging from approximately 1/20° at 80S to 1/4° at 30S. A discussion of the aliased high frequency errors in the Southern Ocean is given by Morrow *et al.* (2003). The altimetry data resolves wavelengths greater than 150 km, with a temporal resolution of 20 days (Ducet *et al.*, 2000). In the Southern Ocean where the groundtracks converge, we can resolve 100 km wavelengths.

Two kinds of simulations have been performed, both lasting one year. In the first case we released virtual drifters at the same time and position as the real drifters. In the second simulation, we released virtual drifters on a regular half-degree grid (roughly 50-100 km) over the whole Southern Ocean, from 30S to 70S. In this latter simulation we launched these virtual drifters in summer and in winter, to better represent the whole seasonal cycle of eddy energy. This simulation is demanding in terms of computing time, so results were obtained only for the year 2000. Drifter pairs were obtained from the same simulation, hence their initial separation is already at the mesoscale. Simulations have been performed with and without mean flow. The mean flow was estimated from two climatological mean dynamic height products: one relative to 1500 m (ship and Argo float database; Sallée *et al.*,

5. http://www.aoml.noaa.gov/phod/dac.html
6. Mean currents available at http://www.aoml.noaa.gov/phod/dac/drifter_climatology.html

2008b) and one from the mean sea surface of Rio *et al.* (2005). Both gave similar results, but we preferred the Sallée *et al.* (2008b) climatological database since more Argo data are incorporated in the Southern Ocean, and smaller spatial scales are resolved.

c. Wind data

In order to simulate drifters advected only in the Ekman flow, we have constructed weekly maps of Ekman velocity at 15 m, which is the depth of the drogued GDP drifters. We used the parameterization proposed by Van Meurs and Niiler (1997) to derived Ekman velocities at 15 m from wind stress:

$$u_e + i v_e = B \exp^{i\theta}(\tau^x + i\tau^y) \tag{6}$$

where the amplitude $B \simeq 0.3$ m s^{-1} Pa^{-1} and θ is the turning angle relative to the wind direction: 55° to the left of the wind in the southern hemisphere at 15 m depth. Wind stress (τ^x, τ^y) is in Nm^{-2}. The value of the turning angle of 55° proposed by Van Meurs and Niiler (1997), has recently been tested by Sudre and Morrow (2008) with a denser drifter dataset, and they found a good visual fit with the *in-situ* data. The resulting Ekman currents at 15 m depth U_e (u_e, v_e) are:

$$u_e = B[\tau^x.\cos(\theta) - \tau^y.\sin(\theta)] \tag{7}$$

$$v_e = B[\tau^x.\sin(\theta) + \tau^y.\cos(\theta)]. \tag{8}$$

We use the Quickscat Mean Wind Field (QSCAT MWF) gridded product for the wind stress (τ^x, τ^y). This global half-degree resolution product provides daily and weekly wind stress fields, and is processed and distributed by the Centre ERS d'Archivage et de Traitement (CERSAT).[7] We used the weekly maps available between July 1999 and March 2007 to simulate virtual drifters released at the same time and position as the real drifters.

d. Data filtering and mapping

We aim to map the dispersion coefficient $\kappa_\infty^{(1)}$, as well as the typical Lagrangian eddy scales, T and L, in the Southern Ocean by applying the previously presented formulations to the surface drifters. This type of calculation requires a series of modifications and particular care. The main problem is averaging over sparsely distributed drifters. In most geophysical experiments, and especially in the present case with surface drifter data, the drifters are deployed at different locations and at different times. Since the oceanic flow is neither homogeneous nor stationary, the averaging procedure is important to document. The following discussion presents some of the solutions we have chosen in this study.

We have divided the total domain area into bins (Davis, 1991), with the size of these bins chosen to approximate homogeneous statistics. Lagrangian scales were calculated from

7. http://www.ifremer.fr/cersat/en/documentation/manuals.htm

non-overlapping 90-day segments of the float trajectories and binned in 5° longitude by 1° latitude bins. The choice of these time and space scales is based of the typical size of an eddy loop along the trajectories. We consider these scales to be larger than the typical scale of energetic eddies but small enough to resolve substantial large-scale variability.

The mean flow is estimated over the duration of the GDP drifter experiment, approximatively 10 years in the Southern Ocean (between 1995 and 2005) for the bulk of the drifters. Since a seasonal mean has been removed from the GDP drifters, the mean flow is defined independently for each season and over 10 years. For the virtual drifters computed from altimetry velocities, a different mean is used: a 7-year altimetric mean from 1993 to 1999 without seasonal considerations (see Section 3b).

Figure 1a shows the dispersion calculated in the ACC sector, between the Polar Front (PF) and the Northern branch of the Subantarctic Front (SAF-N) using the frontal definitions of Sallée *et al.* (2008b). Two regimes are detected: one a transition time with periods less than approximately 50 days where dispersion growth quadratically, and a second regime where the dispersion converges towards linear growth. In this paper we focus on the linear regime. The linear growth regime starts at around 50 days. Furthermore, previous Southern Ocean studies have shown that periods between 40h and 90 days account for most of the eddy signal (Nowlin *et al.*, 1985 in Drake Passage; Phillips and Rintoul, 2000 south of Australia). Thus we chose to filter the residual velocity fields to remove periods greater than 90 days. We note, however, that filtering periods of greater than 90 days (150 days was also tested) does not significantly change our results (not shown). This, together with a low-pass filter to remove energy at periods smaller than two days was applied to both the GDP and virtual drifters, and limits the error introduced by using a different mean definition for each dataset. The filtering also limits the dynamical range and constitutes a second operational definition of the dominant mesoscale flow scales responsible for diffusion. We found that band-passing the velocity in this way accelerates the decorrelation of the dispersion, consistent with studies by Bauer *et al.* (2002).

Many studies have shown that the ACC is strongly steered by the topography (eg. Moore *et al.*, 1999; Dong *et al.*, 2006; Sallée *et al.*, 2008b), due to the topographic β-effect (e.g. LaCasce, 2000; Sinha and Richards, 1999). Since our main interest is in cross-frontal eddy diffusion it is important to attempt to separate the along-stream and cross-stream components. For each bin we have calculated the principle axes of the current (eigenvalues of velocity covariance) and derived the eddy diffusivity in the major and minor axis directions, to distinguish directions of weaker and stronger mixing. The minor axis diffusivity is retained as the estimate of cross-ACC mixing, and the major axis as the estimate of the along-stream ACC mixing. Figure 2 shows the EKE ellipses in the Southern Ocean from the drifter dataset, which are similar to those of Ducet *et al.* (2000) and Morrow *et al.* (1994).

Auto-correlation functions were calculated over the time $T_m = 90$ days, a time scale suggested by Figure 1a as a good compromise. In our calculations, we only keep trajectories that are longer than T_m; the median duration of all retained trajectories is 135 days.

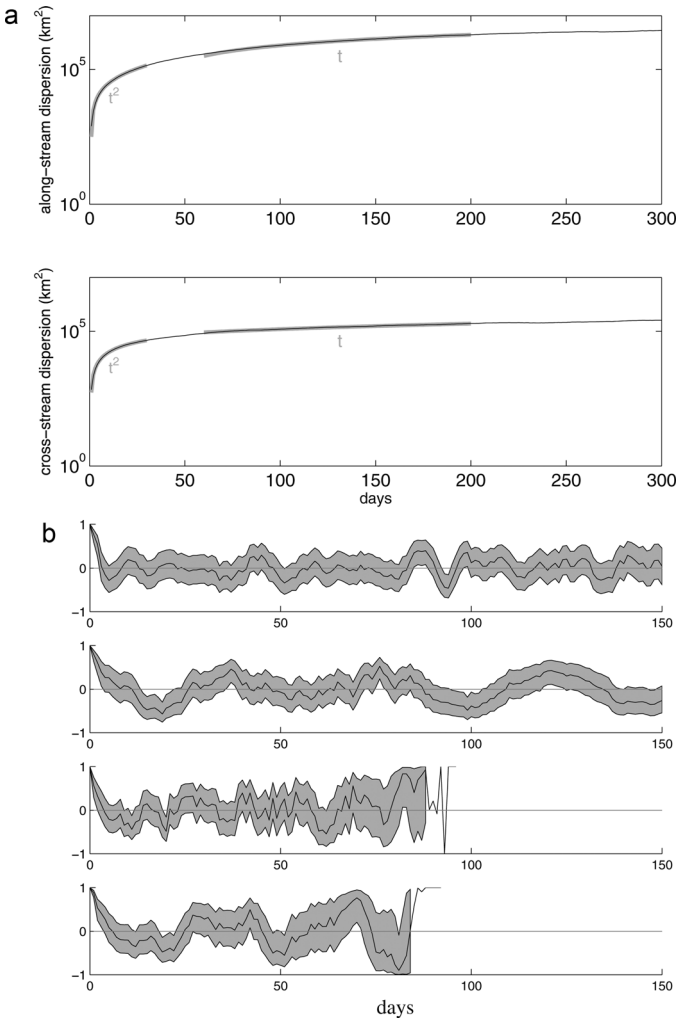

Figure 1. (a) Along- and cross-stream dispersion (km^2) in the ACC around the circumpolar belt from unfiltered surface drifter trajectories. Linear and quadratic regimes are indicated. (b) Examples of autocorrelation function and associated 95% confidence limit for two long and two short trajectories.

Shorter trajectories will have larger errors. Figure 1b shows four examples of autocorrelation functions and their associated 95% confidence limit. The calculation of the diffusive time scale, T, is based on the integration of R, hence may be dominated by noise. However, standard methods have been developed to reduce the noise problem. For example, R can be integrated up to a constant lag (see Speer *et al.*, 1999) or up to the first zero crossing (e.g. Freeland *et al.*, 1975; Poulain and Niiler, 1989). In the Southern Ocean, both of these

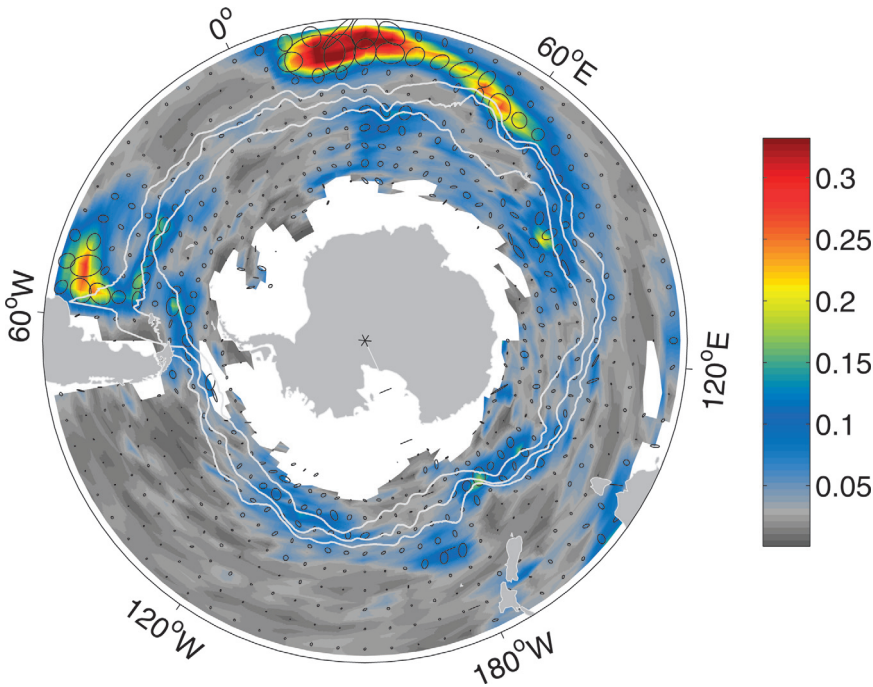

Figure 2. EKE (in $m^2\ s^{-2}$) in the Southern Ocean from GDP drifter data. Ellipses of velocity covariances are superimposed in black.

methods produce noisy fields and have undesirable characteristics (T values which are a function of the constant lag, or inappropriately small values of T, etc.). In this study, we have adapted a method developed by Garraffo *et al.* (2001). In the calculation of T we fit an autocorrelation function of the form:

$$R^* = \cos\left(\frac{\pi\tau}{2Td}\right) e^{-(\tau/\tau_e)} \tag{9}$$

to the observed R. Td is the first zero crossing of R and the e-folding timescale τ_e is found by a least squares method. Then we can compute the exact integral of the R^* function to infinite lag to obtain the integral time scale T:

$$T = \int_0^\infty R^*(\tau)d\tau = \frac{\sqrt{\pi}}{2}\tau_e e^{-(\pi\tau_e/4Td)^2}. \tag{10}$$

This method is strongly constrained by the rapid decrease at early lag hence is not compromised by the large errors on shorter trajectories (see Fig. 1b).

In order to estimate error we used a Monte Carlo method. For each bin, we have a set of autocorrelation functions from the drifters' trajectories from which we derive a mean

autocorrelation function and its standard deviation. We then randomly generate 500 functions within the window formed by the mean autocorrelation plus or minus two standard deviations, and fit R^* to each of these 500 randomly chosen functions. Using R^*, we calculated 500 values of the integral time scale: T_{exp} providing both an average T and its standard error. This generates a standard error on κ of approximatively 1%. The standard deviation is larger, around 28%, but the general structure of the eddy diffusion coefficient remains within the standard deviation limit. These values stand for both the along- and cross-stream coefficients. A variability at seasonal timescales of around 10-15%, as found by Schuckburgh *et al.* (2008a), could explain part of this standard deviation.

4. Results

Figure 3 shows the eddy diffusivity κ calculated with Eq. 2, and the associated eddy time and length scales for the Southern Ocean for both the cross- and along-stream components. The patterns of the cross- and along-stream components are comparable, although the along-stream components show larger values. The largest values are found in the vicinity of the highly energetic currents, mainly near the western boundary currents. Diffusion peaks in the Agulhas Retroflection north of the ACC, between 30E and 70E, and in the southwestern Atlantic in the Brazil Current area. Secondary peaks are found along the ACC where it interacts with bathymetry at 30E, 80E, 170E and 220E, and finally west of New Zealand, near 190E, 50S (see also Bryden and Heath, 1985). Diffusion is much weaker in the eastern parts of all gyres and south of the ACC. Along the mean pathway of the ACC, diffusion tends to be weaker, especially the cross-stream component. However we observe exceptions, where the flow passes over shallow bathymetry such as the mid-ocean ridge near (110E), the Macquarie Ridge (150E), fracture zones in the central Pacific Ocean (220E), and the Falkland Plateau (320E). Over these shallow features the eddy diffusivity is larger (Witter and Chelton, 1998).

The large-scale pattern agrees well with previous studies (e.g. Stammer, 1998; Rupolo, 2007; Zhurbas and Oh, 2004). However, we find slightly higher amplitudes in all of these regions (see Table 1). We note that Marshall *et al.* (2006) found much smaller values of surface diffusion although they resolve similar time scales. Our calculation is based on Lagrangian drifter statistics and gives information about the particle dispersion, whereas their study by construction produced circumpolar integrated measures of tracer transport and an inferred net diffusivity based on tracer gradient budgets in tracer coordinates. After averaging along streamlines we find values closer to theirs, within a factor of 2-5 (Fig. 4). Shuckburgh *et al.* (2008b) recently extended Marshall *et al.*'s (2006) method to produce local values of the diffusion in the South Pacific. They found values very similar to ours, especially in the energetic western Pacific.

High values of eddy diffusion in the surface layer, as we find here, appear to be consistent with coarse climate model simulations. Recent modeling studies suggest a vertical dependence of the diffusivity similar to the stratification, i.e. large in the upper ocean and small

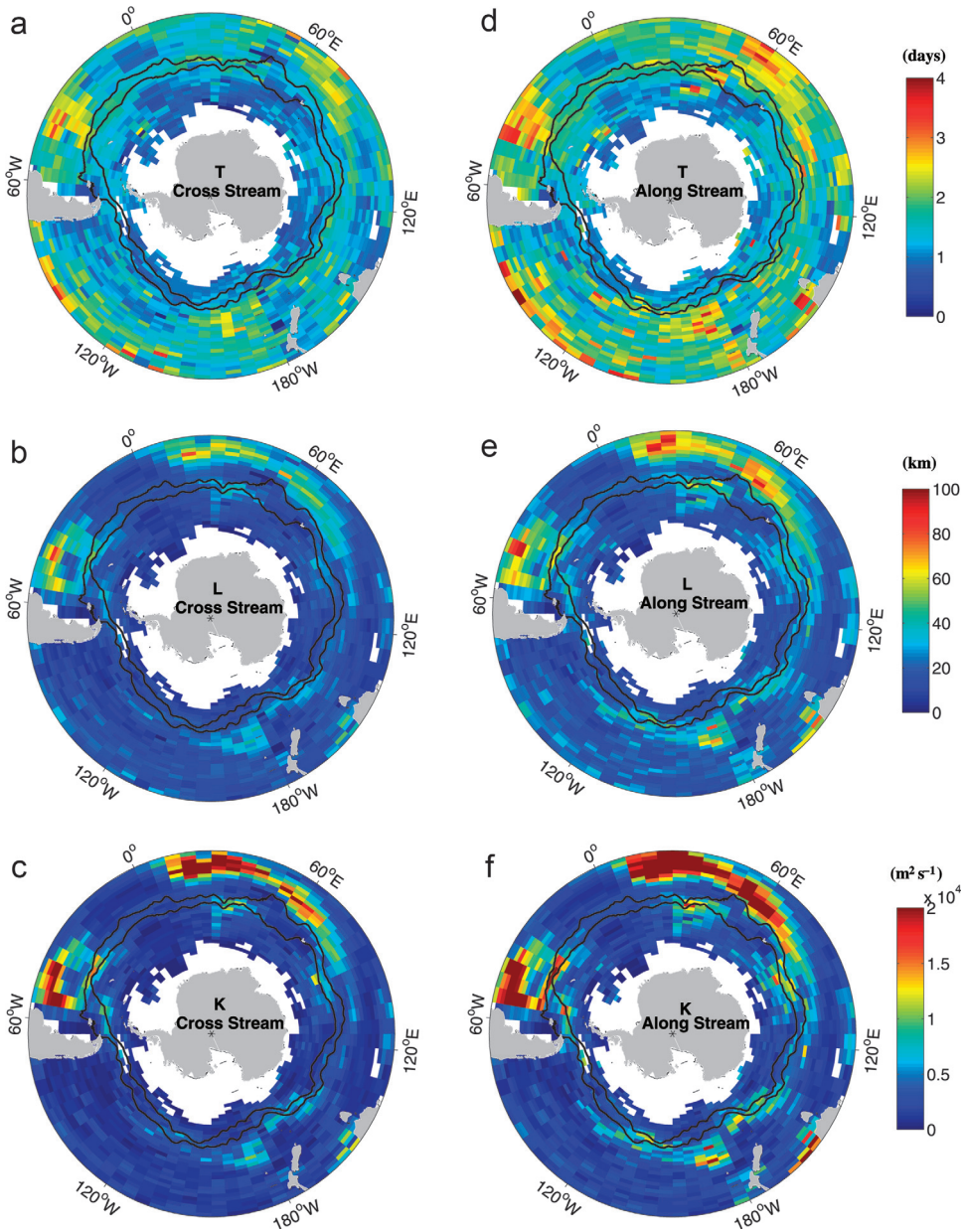

Figure 3. Cross- and along-stream eddy scales in the Southern Ocean from GDP drifter data. Black lines are the mean SAF and PF from Sallée *et al.* (2008b). (a) Lagrangian cross-stream eddy time-scale in days. (b) Lagrangian cross-stream eddy length-scale in km. (c) Cross stream eddy diffusivity coefficient in $m^2\ s^{-1}$. (d) Lagrangian along-stream eddy time-scale in days. (e) Lagrangian along-stream eddy length-scale in km. (f) Along-stream eddy diffusivity coefficient in $m^2\ s^{-1}$.

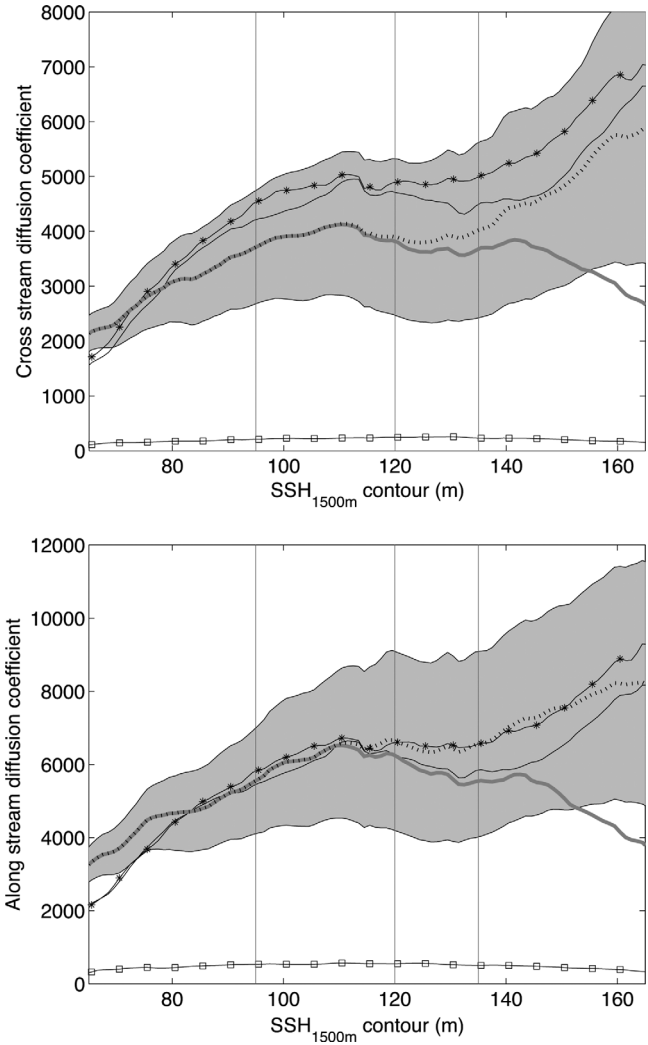

Figure 4. Circumpolar along-stream average of the (a) cross-stream and (b) along-stream eddy diffusion coefficient for different drifter datasets. The coefficients are shown using real in-situ drifters datasets (dotted line, with the associated error shaded). Also shown are the results when the western boundary regions are eliminated (Thick gray line). For comparison, the diffusion computed from particles released on the same grid as the real drifters is shown (thin solid line) along with the diffusion computed from particles released on a regular half degree grid (solid line with star markers). The diffusion induced by virtual drifter trajectories released on the same grid as the surface drifter but advected only by the Ekman velocity is much smaller (open squares). Vertical lines represent the PF , the SAF and the northern branch of the SAF.

Table 1. Approximate values of the eddy diffusivity coefficient ($m^2\ s^{-1}$) extracted from previous studies and compared to the cross stream eddy diffusion coefficient of our present study. Stammer (1998) applied a 0.1 factor to his results to transform calculated surface values to a vertically averaged value; we remove this factor and display the surface value for a more consistent comparison.

	Agulhas Retroflection	Brazil Current	Campbell Plateau	East of New Zealand
Stammer (1998)	1.10^4	1.10^4	1.10^4	–
Zhurbas and Oh (2004)	$2-3.10^4$	$1.5-2.10^4$	1.10^4	$0.6-0.8.10^4$
Rupolo (2007)	$2-3.10^4$	2.10^4	$1.5.10^4$	1.10^4
Our Study	$2-3.10^4$	2.10^4	$0.5-1.10^4$	1.10^4

in the abyss (Ferreira *et al.*, 2005). Based on this idea Danabasoglu and Marshall (2007) used a surface diffusivity as large as 4000 m^2/s on zonal average, much like our value, and with a spatial pattern similar to ours. They found it significantly improves the simulation of the upper ocean in their model.

a. Simulations

We used simulations to assess sampling errors in our calculation. In a first experiment we launched virtual drifters at the same place and time as the real GDP drifters and computed eddy scales. We found very similar time, length and diffusion scales (not shown). The patterns and intensities of the diffusion found with real drifters or with simulated drifters are comparable. The simulated drifters are only advected by the geostrophic mean flow and the quasi-geostrophic mesoscale eddies captured by altimetry. The fact that there is reasonable agreement with the in-situ data suggests that the calculation presented in Figure 3 is dominated by mesoscale eddy activity and the mean flow, and that there is not significant aliasing of small-scale phenomena by the band-pass filtered real drifters. This suggests that the resolved geostrophic flow is the main contributor to the observed eddy diffusion.

In the second experiment we launched virtual drifters on a regular half-degree grid, first in winter and then in summer and let them drift for one year. Once again, we found results in very good agreement with the real data estimates of eddy scales. Intensities remain within the standard deviation limit of the real drifter experiment. In order to assess the role of the mean flow on the diffusion, we ran a third simulation with no mean flow. In this latter experiment, the drifters evolved only with the anomaly of the geostrophic flow.

Figure 4 shows a stream-wise circumpolar average of the different calculations. On average over the circumpolar belt, the real data and the simulated drifter calculations give similar results. The general pattern revealed by an along-stream average is: (1) an increase of the diffusion from Antarctica to the Subantarctic Front (SAF); (2) a local minimum or a plateau of diffusivity across the northern side of the ACC (around SAF, SAF-N); (3) and an increase in the diffusion north of the ACC in the western boundary current regions.

A local minimum of diffusivity in a front (Bower *et al.*, 1985; Haynes *et al.*, 2007) or in the ACC (Marshall *et al.*, 2006; Shuckburgh *et al.*, 2008b) has been previously observed,

and attributed to the high potential vorticity (PV) gradient associated with the jets. In our study we do not observe a significant reduction in the mixing within the jet. We note, however, that our circumpolar averaging does not follow the instantaneous jet's high PV gradient, as opposed to that of Marshall *et al.* (2006). For example, if a jet undergoes a large nonsteady meander, and we average along the mean streamfunction, we would average values of diffusion computed inside and outside the high gradient region of the jet. Conversely, the Nakamura (1996) calculation performed by Marshall *et al.* (2006) produces, by construction, an eddy diffusion coefficient averaged both in time and space along the instantaneous streamline. Marshall *et al.*'s (2006) method provides an accurate description of the net circumpolar effect of eddy mixing, with accurate cross-mean tracer field resolution. On the other hand, it combines very different regimes, western boundary current, topographic, and interior, into this estimate.

As opposed to Marshall *et al.* (2006) we found little change in the circumpolar averaged diffusion without the mean flow. We observed a slight reduction of the diffusion for both along- and cross-stream calculation, but this reduction is small compare to the error of the calculations. However, consistent with Shuckburgh *et al.* (2008b) we observe significant local increases of the diffusion within the ACC when removing the mean flow, especially in regions where the mean flow intensifies (e.g. flow through fracture zones, over the Southwest Indian Ridge near 30E; or in the area from 120–130E). These local increases of several thousands of $m^2\ s^{-1}$ vanish in the circumpolar average.

We also simulated drifter trajectories using the Ekman currents at 15 m in order to assess the contribution of Ekman in the diffusivity calculation. Diffusion maxima are now found in the vicinity of the ACC, in the Indian and Pacific basin where the wind is the most powerful and variable (Trenberth *et al.*, 1990; Luis and Pandey, 2004). The intensity of the diffusion is also much weaker, roughly one order of magnitude less than the geostrophic mesoscale eddy contribution. An along-stream average of the diffusion due to the Ekman velocities (Fig. 4) shows that Ekman contribution to the eddy diffusivity at 15 m is negligible compared to the contribution of geostrophic mesoscale eddies.

Finally, drifters tend to converge toward the very diffusive regions (Davis, 1991), which could bias our results. However, the difference between the calculation on the regular and on the sparse grid remains within the standard deviation limit of the real drifter experiment, hence we believe this theoretical bias does not significantly affect our results. Note that there is another possible source of divergence between regular and sparse grid experiment. Any interannual increase (Meredith and Hogg, 2006) in the eddy activity may cause slight differences in the results in the energetic regions.

b. Absolute and relative dispersion

We have calculated the probably density function (pdf) of the particle velocities and their absolute dispersion (see Eq. 4), and also derived κ from this using the explicit formulation (Eq. 1). Figure 5 shows the results for the ACC (between Polar and northern Subantarctic

Fronts) together with an estimate of the relative dispersion computed from the explicit formulation (Eq. 5). We note that the absolute dispersion, and consequently the absolute diffusion, computed with the explicit equation (Eq. 1) are both very smooth since we fit an idealized function to the observed autocorrelation function before calculating these terms. These results are also in good agreement with the coefficients found with the real drifter trajectory data. Interestingly, when the mean flow is removed (Fig. 5c,f) there is very little impact on the results.

Departures from a Gaussian distribution are found at small and large velocities (Fig. 5b,e) similar to Bracco *et al.* (2000). The departure from the expected Gaussian shapes are thought to be associated with the action of energetic coherent structures that introduce extreme velocities (Bracco *et al.*, 2000). We note that the pdf from simulated drifters is very close to the pdf found with real velocity data: the observed departure from Gaussian shape in the ocean can be explained by the quasi-geostrophic mesoscale eddies resolved by altimetry. Around the circumpolar belt, in bins of 5° longitude by 1° latitude, we found a sharp

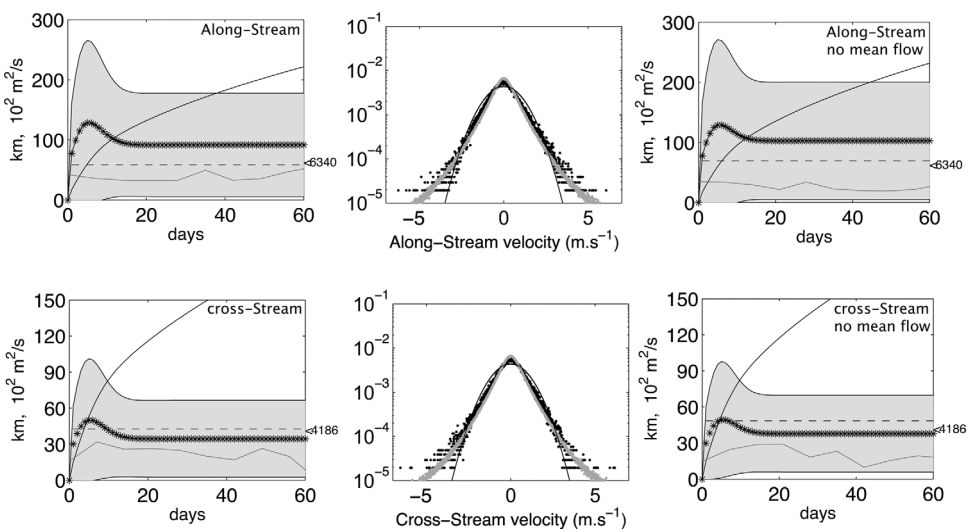

Figure 5. (a) Absolute along-stream dispersion of particles (square root, in km) in the ACC (between the PF and the SAF-N) calculated from the simulated drifters on a half degree regular grid with mean flow. The explicit absolute diffusion is given (stars) with its standard deviation (grey envelope). The limit at infinity of the implicit absolute diffusion ($\kappa_{\infty}^{(1)}$) is also marked (dashed line). The evolution of the relative diffusion divided by two is superimposed (grey line; 1/2 $\kappa^{(2)}$). (b) Pdf of the along-stream velocities used in panel a (black points). Also shown is the pdf of the real in-situ drifter along-stream velocities over the same area (grey points). The black line represents a Gaussian envelope. Panel (c) is the same as panel (a) but for a simulation without the mean flow. Panels (d), (e) and (f) correspond respectively to the panels (a), (b) and (c) but for the cross-stream componenent.

distribution of kurtosis centered on 5.5 (not shown), which reveals that a departure from Gaussian occurs nearly everywhere in the Southern Ocean, with a slightly larger departure near the western boundary currents.

c. Relation to EKE

The formulation of a climatological eddy diffusion map with its distinct geographical distribution is a first step in parameterizing eddy mixing in the Southern Ocean. However, the calculation is difficult to replicate because of somewhat subjective averaging procedures, geographical bin size choices, etc. Of further interest would be to use these results to calibrate a simpler calculation directly from the altimetry observations themselves. In addition, we cannot use these results to study a time evolution of the diffusivity without waiting for many more drifter deployments. In this Section we investigate whether a simple parameterization can be developed which relates the scales of motion of an altimetry-based random velocity field to the cross-stream eddy diffusion in the Southern Ocean. Note that in this section we only investigate the parameterization of the cross-stream coefficient (e.g. Middleton, 1985; Lumpkin *et al.*, 2002; Chiswell *et al.*, 2007).

When a float passes through an eddy field its displacement (Lagrangian) is influenced by both the spatial and length scales of the eddy field (Eulerian). There is *a priori* no reason for the Eulerian and Lagrangian time scales (respectively T_E and T) to be easily related. However, Middleton (1985) found that the ratio $\eta = T_E/T$ could be determined within 10% by an empirical equation. This equation is given in terms of the ratio u_{rms}/c^*, where c^* is the ratio of the Eulerian length scale (L_E) over the Eulerian time scale (T_E).

Considering extreme regimes helps to understand the existence of a relation between Eulerian and Lagrangian scales. If a float drifts through a small portion of an eddy before the eddy field significantly change, i.e. $L \ll L_E$, then one can say that the float is almost fixed compare to the eddy field. Its sampling can be compared to the sampling of a current meter: the temporal decorrelation of its velocity is due to the temporal decorrelation of the eddy field. Hence, in this *fixed float regime* $T_E \approx T$. At the other extreme if a float drifts through many eddies before the eddy field significantly change, i.e. $T_E \ll T$, then eddy size determine the float trajectory's meanders. Hence, in this *frozen field regime* $L_E \propto L$. If oceanic drifters uniformly encounter one of these two regimes, then one could use the Eulerian measurement to assess the eddy diffusivity. In this section we assume that a relation does exist between Eulerian scales and diffusivity and check a-posteriori the consistent of this assumption versus our previous Lagrangian based estimation.

The eddy diffusion coefficient is basically the product of a typical eddy velocity, U_e multiplied by a typical eddy length scale, L_e. Since Stammer (1998)'s results supported a correlation between the dominant eddy scale and the deformation radius, we approximated L_e by the baroclinic Rossby deformation radius, L_d. Finally, a measure of the typical eddy velocity is the square root of the eddy kinetic energy, $\sqrt{EKE}$. Then, we have:

$$\kappa^{(1)} = \langle u'd' \rangle = \alpha\sqrt{EKE}L_d, \tag{11}$$

where α is a proportionality constant. Stammer (1998) used this parameterization to calculate the diffusion in the Southern Ocean with altimetry, and applied a fixed coefficient $\alpha = 0.05$. In this study, we recalculated the coefficient α using our climatological eddy diffusion map from the Lagrangian drifters and compared it to EKE from altimetry over the same period.

Figure 6a shows a map of the distribution of this coefficient α. We used the internal baroclinic Rossby radius L_d, calculated from climatological hydrographic data by Chelton *et al.* (1998).[8] We found that values of α are quite stable in the energetic areas of the Southern Ocean (Fig. 6b). A clear mode shows up in the histogram of α in the bins where EKE exceeds 0.015 $m^2\ s^{-2}$. The relatively sharp distribution of the α coefficient in these energetic regions justifies choosing a simple parameterization. In the lower energy regions we cannot apply a simple parameterization, because the Lagrangian integral length scale becomes uncorrelated with the Eulerian length scale given by altimetry. The regions where this simple parameterization holds are concentrated in the western boundary currents, and in the energetic ACC. An area of approximatively 2.10^7 km^2 is concerned, which represents 30% of the total area of the Southern Ocean. Over the rest of the Southern Ocean, the eddy field is weaker and the mixing is fairly uniform at about 1800 ± 1000 $m^2\ s^{-1}$. Finding a nearly constant α coefficient over the energetic ACC region implies that there is a proportional relationship between the Lagrangian and Eulerian length scales, i.e. that the energetic ACC region is in the *frozen field regime*. Thus, with respect to Lagrangian sampling, the ACC is similar to the highly energetic near-surface Gulf-Stream (Lumpkin *et al.*, 2002). We chose the median value of this distribution for EKE ≥ 0.015 $m^2\ s^{-2}$ as the better estimate of the parameterization: $\alpha = 1.35$. This value is approximately 27 times greater than derived by Stammer (1998). We note, however, that our eddy diffusion values are of the same order since Stammer (1998) used a much greater baroclinic Rossby radius than ours.

Stammer (1998) assumes a proportional relationship between the Lagrangian and Eulerian length scales everywhere in the Southern Ocean, which we have shown to be only true in the energetic areas along the ACC and in the western boundary currents. Outside these energetic regions, a constant value of α times $\sqrt{EKE}.L_d$ would give an overestimate of the diffusion. In the energetic areas, the simple relation using a recalibrated coefficient of proportionality allows one to map and monitor the eddy diffusion in the Southern Ocean using the time series of altimetric data maps.

5. Discussion

The along- and cross-stream eddy diffusion coefficients have been determined using the newer, denser dataset of GDP drifters available in the Southern Ocean. We computed the statistics of drifter observations to find an estimate of these coefficients in different regions.

8. www.coas.oregonstate.edu/research/po/research/chelton/index.html

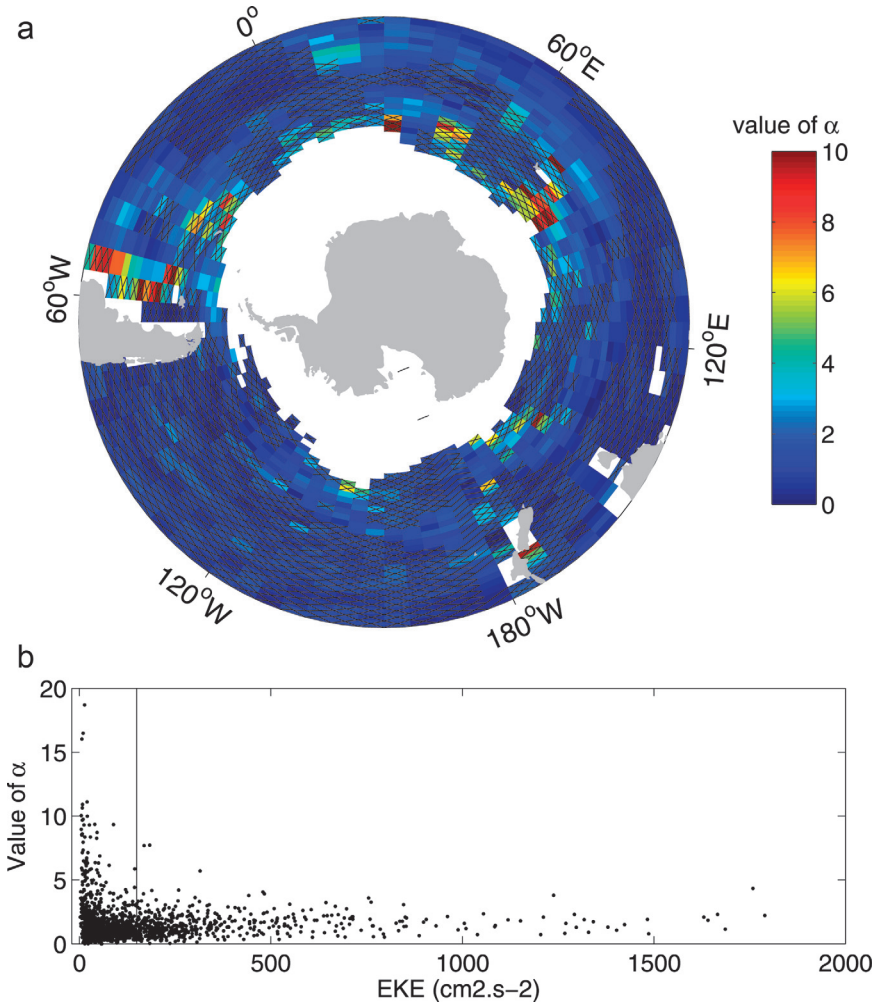

Figure 6. Result of the calibration of the proportionality coefficient α used in the parameterization of the eddy diffusion coefficient: $\kappa = \alpha.\sqrt{EKE}L_d$. (a) geographical distribution. Crosshatching indicates areas where EKE is less than 0.015 $m^2\ s^{-2}$. (b) Value of the coefficient α as a function of the EKE. The vertical line represents EKE = 0.150 $m^2\ s^{-2}$.

We found that the surface layer of the Southern Ocean is significantly diffusive, with maxima concentrated in the main western boundary currents, such as the Agulhas Retroflection or the Brazil current, and also east of New Zealand. Intrinsic errors such as small scale aliasing or sampling errors were quantified using simulated drifter datasets. The mean flow reduces the diffusion locally in a few regions of enhanced mean flow within the ACC, but we do not observe a circumpolar-averaged reduction.

The high values of near surface diffusivity found here will strongly mix tracers in the surface mixed layer, but the strongest mixing is confined to relatively small regions of the Southern Ocean. A measure of this inhomogeneity is that the median values of cross-stream κ in the ACC are approximatively 3000 $m^2\ s^{-1}$, substantially lower than the average values (around 4000 $m^2\ s^{-1}$). These lower values are more representative of what a tracer experiences; however, this does point to the fact that no single value represents tracer diffusion globally.

Marshall *et al.* (2006) found values of diffusion much smaller than ours. They use a method developed by Nakamura (1996), which is widely used in atmospheric sciences. The differences in the resulting diffusivity when using either the Nakamura (1996) or the Taylor (1921) method are significant and intriguing. We note here some differences in the two approaches.

First, the Nakamura (1996) method depends on the detailed deformation rate of a tracer. Reversing flow structures like a large-scale meanders do not contribute to mixing. Hence, the resulting diffusion is computed with an effective high spatial-scale resolution. In our calculation the drifters are coarsely distributed and effectively averaged over streamlines, resulting in an overestimate of cross-stream diffusion. Both studies made use of altimetry-derived velocities, which based on our comparison with real drifters adequately represents the eddy flow responsible for diffusion. Since Marshall *et al.* (2006) note that the value of the diffusion is not significantly affected when they change their resolution from 1/4 to 1/100 degree, the differences between the results do not appear to be due to resolution, but to the methodology. Secondly, Marshall *et al.* (2006) evolve their tracer field by an advection-diffusion equation that depends on the choice of the explicit mixing. Therefore, the different results may not be significant when all sources of error are taken into account. A sensitivity experiment shows that the choice of explicit mixing can change the resulting effective diffusivity, by as much as a factor of two or so.

The Nakamura (1996) calculation performed by Marshall *et al.* (2006) gives a circumpolar integrated value of the effective diffusivity, and does not resolve the circumpolar structure of the diffusion. Their circumpolar map is a projection of an integrated value and cannot be directly compared with our circumpolar map. In our calculation we average the diffusion over a geographic bin followed by an average over the circumpolar path. Marshall *et al.* (2006) calculate circumpolar values by construction. The recent study by Shuckburgh *et al.* (2008b) uses the Nakamura (1996) approach to compute the diffusion in geographical bins in the South Pacific, avoiding circumpolar integrated values. They find local peaks of diffusivity within the ACC and values of diffusion much closer to ours, for example around 5000 $m^2\ s^{-1}$ in the eastern South Pacific. Recently it has been suggested that increasing the eddy diffusion coefficient in the surface layer of a climate model to values similar to these gives a reasonable representation upper ocean (Danabasoglu and Marshall, 2007).

In addition, we use a streamfunction computed from the recent and numerous Argo data, which better resolves smaller scales, and especially the large steady meanders of the ACC along its path. Marshall *et al.* (2006), like many other previous studies, use a very smoothed

streamfunction. Their streamfunction is much more like a zonal average, and when we zonally average our results we find a pattern somewhat closer to theirs, with peak diffusion near 60 S, and a local minimum between 50 S and 55°S (not shown). It is less clear how this structure is related to frontal position, though, in this average.

A simple parameterization based on the scales of motion resolved by altimetry may usefully represent the explicit cross-stream diffusion estimated from surface drifters in the energetic areas of the Southern Ocean. In these regions, we propose a parameterization similar to that of Stammer *et al.* (1998), but with a recalibrated proportionality coefficient based on our drifter results. Outside these regions diffusion does not vary significantly. As found by Lumpkin *et al.* (2002) for the high energetic surface Gulf Stream regions, in the energetic portions of the ACC the eddy field is in the "frozen field" regime. In this regime a simple parameterization can exist and implies a proportional relationship between Lagrangian and Eulerian length scales. Such a parameterization could allow one to monitor interannual variability of the diffusion in the energetic areas via altimetry or other observations of geostrophic flow.

Meredith and Hogg (2006) observed an increase of EKE in the Southern Ocean from altimetric data. They showed that the mechanisms leading to such a low frequency EKE variability could be a delayed response to atmospheric circulation changes. Our parameterization shows that an interannual increase of the EKE could be associated with an increase of the diffusion in the energetic sector of the Southern Ocean, consistent with the recent modeling study by Hogg *et al.*, (2008). A delayed lateral diffusive heat flux response may contribute to low-frequency variability in mode waters (Sallée *et al.*, 2008a) and other water masses in the Southern Ocean. That this heat flux and warming may occur preferentially in regions where the EKE lies above some threshold may explain why warming has not been observed everywhere (Gille, 2002) but rather with a regional dependence.

Acknowledgments. Drifter data are quality controlled, interpolated, and distributed by NOAA's Global Drifter Program, http://www.aoml.noaa.gov/phod/dac/gdp.html. Drifter deployments are coordinated with numerous national and international partners. The Argo data were collected and made freely available by the International Argo Project and the national programs that contribute to it (http://www.argo.ucsd.edu, http://argo.jcommops.org). Argo is a pilot program of the Global Ocean Observing System. KGS received support from NSF OCE-0336697 Climate Process Team CPT-Emilie and the Laboratoire d' Etudes en Geophysique et Oceanographie Spatiale. Funding for this study comes from the French PATOM and TOSCA programs. RL received support from NOAA's Atlantic Oceanographic and Meteorological Laboratory.

REFERENCES

Batchelor, G. and A. Townsend. 1956. Surveys in Mechanics: A Collection of Surveys of the Present Position of Research in Some Branches of Mechanics, Cambridge Univ. Press, 352–399.

Bauer, S., M. Swenson and A. Griffa. 2002. Eddy mean flow decomposition and eddy diffusivity estimates in the tropical Pacific Ocean: 2. Results. J. Geophys. Res., *107(C10)*, 3154.

Bennett, A. 1984. Relative dispersion: local and nonlocal dynamics. J. Atmos. Sci., *41*, 1881–1886.

—— 1987. A Lagrangian analysis of turbulent diffusion. Rev. Geophys., *25(4)*, 799–822.

Bower, A. S., H. Rossby and J. Lillibridge. 1985. The Gulf Stream - barrier or blender? J. Phys. Oceanogr., *15*, 24–32.

Bracco, A., J. LaCasce and A. Provenzale. 2000. Velocity probability density functions for oceanic floats. J. Phys. Oceanogr., *30*, 461–474.

Bryden, H. and R. Heath. 1985. Energentic eddies at the northern edge of the Antarctic Circumpolar Current in the southwest Pacific. Prog. Oceanogr., *14*, 65–87.

Chelton, D., R. deSzoeke, M. Schlax, K. Naggar *et al.* 1998. Geographical variability of the first baroclinic Rossby radius of deformation. J. Phys. Oceanogr., *28*, 433–460.

Chiswell, S., G. Rickard and M. Bowen. 2007. Eulerian and Lagrangian eddy statistics of the Tasman Sea and southwest Pacific Ocean. J. Geophys. Res., *112*, C10004.

Danabasoglu, G. and J. Marshall. 2007. Effects of vertical variations of thickness diffusivity in an ocean general circulation model. Ocean Model., *18*, 122–141.

Davis, R. 1982. On relating Eulerian and Lagrangian velocity statistics: Single particles in homogeneous flows. J. Fluid Mech., *114*, 1–26.

—— 1991. Lagrangian ocean studies. Annu. Rev. Fluid Mech., *23*, 43–64.

Dong, S., J. Sprintall and S. Gille. 2006. Location of the Polar Front from AMSR-E satellite sea-surface temperature measurements. J. Phys. Oceanogr., *36*, 2075–2089.

Ducet, N., P. Le Traon and G. Reverdin. 2000. Global high-resolution mapping of ocean circulation from TOPEX/Poseidon and ERS-1 and -2. J. Geophys. Res., *105*, 19,477–19,498.

Ferreira, D., J. Marshall and P. Heimbach. 2005. Estimating eddy stresses by fitting dynamics to observations using a residual-mean ocean circulation model and its adjoint. J. Phys. Oceanogr., *35*, 1891–1910.

Freeland, H., P. Rhines and T. Rossby. 1975. Statistical observations of the trajectories of neutrally buoyant floats in the North Atlantic. J. Mar. Res., *33*, 383–404.

Garraffo, Z., A. Mariano, A. Griffa, C. Veneziani *et al.* 2001. Lagrangian data in a high-resolution numerical simulation of the North Atlantic. I. Comparison with in-situ drifter data. J. Mar. Syst., *29*, 157–176.

Gille, S. 2002. Warming of the Southern Ocean since the 1950s. Science, *295*, 1275–1277.

Hansen, D. and P. Poulain. 1996. Quality control and interpolation of WOCE/TOGA drifter data. J. Atmos. Ocean. Tech., *13*, 900–909.

Haynes, P., D. Poet and E. Shuckburgh. 2007. Transport and mixing in kinematic and dynamically consistent flows. J. Atmos. Sci., *64*, 3640–3651.

Hogg, A., M. Meredith, J. Blundell and C. Wilson. 2008. Eddy heat flux in the Southern Ocean: Response to variable wind forcing. J. Climate, *21*, 608–620.

Keffer, T. and G. Holloway. 1988. Estimating southern ocean eddy flux of heat and salt from satellite altimetry. Nature, *332*, 624–626.

LaCasce, J. 2000. Floats and f/h. J. Mar. Res., *58*, 61–85.

—— 2008. Statistics of Lagrangian observations. Prog. Oceanogr., *77*, 1–29.

LaCasce, J. and A. Bower. 2000. Relative dispersion in the subsurface North Atlantic. J. Mar. Res., *58*, 863–894.

Le Traon, P., F. Nadal and N. Ducet. 1998. An improved mapping method of multisatellite altimeter data. J. Atmos. Ocean. Tech., *15*, 522–534.

Luis, A. and P. Pandey. 2004. Seasonal variability of QSCAT-derived wind stress over the Southern Ocean. Geophys. Res. Lett., *31*, L13304.

Lumpkin, R. and P. Flament. 2001. Lagrangian statistics in the central North Pacific. J. Mar. Syst., *29*, 141–155.

Lumpkin, R. and Z. Garraffo. 2005. Evaluating the decomposition of Tropical Atlantic Drifter observations. J. Atmos. Ocean. Tech., *22(9)*, 1403–1415.

Lumpkin, R. and M. Pazos. 2007. Measuring surface currents with Surface Velocity Program drifters: the instruments, its data and some recent results, *in* Lagrangian Analysis and Prediction of Coastal and Ocean Dynamics. Cambridge University Press.

Lumpkin, R., A. Treguier and K. Speer. 2002. Lagrangian eddy scales in the Northern Atlantic Ocean. J. Phys. Oceanogr., *32*, 2425–2440.

Marshall, J., E. Shuckburgh, H. Jones, and C. Hill. 2006. Estimates and implications of surface eddy diffusivity in the Southern Ocean derived from tracer transport. J. Phys. Oceanogr., *36*, 1806–1821.

Meredith, M. and A. Hogg. 2006. Circumpolar response of the Southern Ocean eddy activity to changes in the Southern Annular Mode. Geophys. Res. Lett., *33*, 2006GL026499.

Middleton, J. 1985. Drifter spectra and diffusivities. J. Mar. Res., *12*, 37–55.

Moore, J., M. Abbott and J. Richman. 1999. Location and dynamics of the Antarctic Polar Front from satellite sea surface temperature data. J. Geophys. Res., *104*, 3059–3073.

Morrow, R., A. Brut and A. Chaigneau. 2003. Seasonal and interannual variations of the upper ocean energetics between Tasmania and Antarctica. Deep-Sea Res. I, *50*, 339–356.

Morrow, R., R. Coleman, J. Church and D. Chelton. 1994. Surface eddy momentum flux and velocity variances in the Southern Ocean from GEOSAT altimetry. J. Phys. Oceanogr., *24*, 2050–2071.

Nakamura, N. 1996. Two-dimensional mixing, edge-formation, and permeability diagnosed in area coordinates. J. Atmos. Sci., *53*, 1524–1537.

Nowlin, Jr, W. D., S. J. Worley and T. Whitworth, III. 1985. Methods for making point estimates of eddy heat flux as applied to the Antarctic Circumpolar Current. J. Geophys. Res., *90*, 3305–3324.

Oh, I., V. Zhurbas and W. Park. 2000. Estimating horizontal diffusivity in the East Sea (Sea of Japan) and the Northwest Pacific from satellite-tracked drifter data. J. Geophys. Res., *105*, 6483–6492.

Owens, W. 1984. A synoptic and statistical description of the Gulf Stream and subtropical gyre using SOFAR floats. J. Phys. Oceanogr., *14*, 104–113.

Patterson, S. 1985. Surface circulation and kinetic energy distribution in the southern hemisphere oceans from FGGE drifting buoys. J. Phys. Oceanogr., *15*, 865–884.

Phillips, H. E. and S. R. Rintoul. 2000. Eddy variability and energetics from direct current measurements in the Antarctic Circumpolar Current south of Australia. J. Phys. Oceanogr., *30*, 3050–3076.

Poulain, P. and P. Niiler. 1989. Statistical analysis of the surface circulation in the Californian Current system using satellite-tracked drifters. J. Phys. Oceanogr., *19*, 1588–1603.

Rio, M., P. Schaeffer, F. Hernandez and J. Lemoine. 2005. The estimation of the ocean mean dynamic topography trough the combination of altimetric data, in-situ measurements and GRACE geoid: from global to regional studies. Proceedings of the GOCINA international workshop, Luxembourg.

Rupolo, V. 2007. A Lagrangian-based approach for determining trajectories taxonomy and turbulence regimes. J. Phys. Oceanogr., *37*, 1584–1609.

Sallée, J., R. Morrow and K. Speer. 2008a. Eddy diffusion and Subantarctic Mode Water formation. Geophys. Res. Lett., *35*, L05607, doi: 10.1029/2007GL032827.

—— 2008b. Response of the Antarctic Circumpolar Current to atmospheric variability. J. Climate, *21*, 3020–3039.

Sallée, J., N. Wienders, R. Morrow and K. Speer. 2006. Formation of Subantarctic mode water in the Southeastern Indian Ocean. Ocean Dyn. *56*, 525–542, doi: 10.1007/s10236–005–0054–x.

Shuckburgh, E., E. Jones, J. Marshall and C. Hill. 2008a. Quantifying the eddy diffusivity of tracers in the ocean: 1. temporal variability in the Southern Ocean. J. Phys. Oceanogr., submitted.

—— 2008b. Quantifying the eddy diffusivity of tracers in the ocean: 2. regional variability in the Southern Ocean. J. Phys. Oceanogr., submitted.

Sinha, B. and K. Richards. 1999. Jet structure and scaling in the Southern Ocean. J. Phys. Oceanogr., *29*, 1143–1155.

Speer, K., J. Gould and J. LaCasce. 1999. Year-long float trajectories in the Labrador Sea water of the Eastern North Atlantic Ocean. Deep-Sea Res. II, *46*, 165–179.

Stammer, D. 1998. On eddy characteristics, eddy transports, and mean flow properties. J. Phys. Oceanogr., *28*, 727–739.

Stewart, R., C. Shum, B. Tapley and L. Ji. 1996. Statistics of geostrophic turbulence in the Southern Ocean from satellite altimetry and numerical models. Physica D., *98*, 599–613.

Sudre, J. and R. Morrow. 2008. Global surface currents: a high-resolution product for investigating ocean dynamics. Ocean Dyn. *10.1007/*, s10236–008–0134–9.

Sybrandy, A. and P. Niiler. 1991. WOCE/TOGA Lagrangian drifter construction manual. Technical report, Tech. Rep. University of California, San Diego, WOCE Report Number 63, 58 pp.

Taylor, G. 1921. Diffusion by continuous movements. P. Lond. Math. Soc., *20*, 196–212.

Trenberth, K., W. Large and J. Olson. 1990. The mean annual cycle in global wind stress. J. Phys. Oceanogr., *30*, 1742–1760.

Van Meurs, P. and P. Niiler. 1997. Temporal variability of the large-scale geostrophic surface velocity in the northeast Pacific. J. Phys. Oceanogr., *27*, 2288–2297.

Witter, D. L. and D. B. Chelton. 1998. Eddy-mean flow interactions induced by modulations of zonal ridge topography in a quasi-geostrophic channel model. J. Phys. Oceanogr., *28*, 2019–2039.

Zhurbas, V. and I. Oh. 2003. Lateral diffusivity and Lagrangian scales in the Pacific Ocean as derived from drifter data. J. Geophys. Res., *108*, 10–1/10–10.

—— 2004. Drifter-derived maps of lateral diffusivity in the Pacific and Atlantic Oceans in relation to surface ciculation patterns. J. Geophys. Res., *109*, 1–10.

Received: *3 August, 2007*; revised: *14 August, 2008*.